Assignment 1

PRADEEP KUMAR BAL

March 22, 2018

Introduction

Damage mechanics is concerned with the representation, or modelling, of damage of materials that is suitable for making engineering predictions about the initiation, propagation, and fracture of materials without resorting to a microscopic description that would be too complex for practical engineering analysis. The term Continuum Damage Mechanics has been used to model materials which are characterized by loss of stiffness, i.e. by a decrease in their stiffness modulus. Damage models have also been used to simulate different materials (fragile and ductile), which are fundamentally characterized by irreversible material degradation. Physically, we can describe the degradation of mechanical material properties as processes in which the initiation and growth (propagation) of micro-defects such as micro pores and micro cracks take place.

Part 1:

(a) The continuum isotropic "non-symmetric tension-compression" damage model:

The non-symmetrical damage model is useful to simulate materials, such as concrete, rocks, whose tension domain differs with respect to compression. The correct modelling of mechanical behaviour of quasi-brittle materials subject to multi-axial tension-compression stress states still represents a challenging theme, especially when the prediction of failure is in point. A key dissipative phenomenon for such materials is certainly micro-cracking which results in non-symmetric, progressive degradation of mechanical properties under tension and compression conditions. A continuum isotropic "non-symmetric tension-compression" damage model has been implemented. The code has been delineated in the Section 1 and 2 of the Annex. The damage surface for the implemented model considering the ratio of the uni-axial elastic limit stress in compression /tension as 3, has been shown below in the Figure 1 with principal stresses axes . It can be clearly observed that the elastic limits of the elastic domain are different for tension and compression.

The "tension-only" damage model:

The tension-only damage model does not take into account failure by compression, i.e. the material can only fail by tension. In this case, the material only loses elasticity due to tension, and we can't find the elastic limit in compression up to infinite. The region in which all the principal stresses are negative, the elastic limit can never be experienced (The damage function f is always negative). The elastic domain is an open domain at infinite for compressive stresses. A "tension-only" damage model has been implemented. The code has been presented in the Section 1 and 2 of the Annex. The damage surface for the implemented model has been depicted below in the Figure 2 (with principal stresses axes). It can be clearly observed that in the third quadrant of the principal stress space, the elastic domain can't be reached up to infinite. In the first quadrant where all the principal stresses are positive, the damage is associated to only the tensile behaviour. For the other two quadrants (II and IV), the elastic limit for the negative part of the principal stresses is located asymptotically at infinite, and for the positive counterpart of the principal stresses, the elastic limit can be reached.

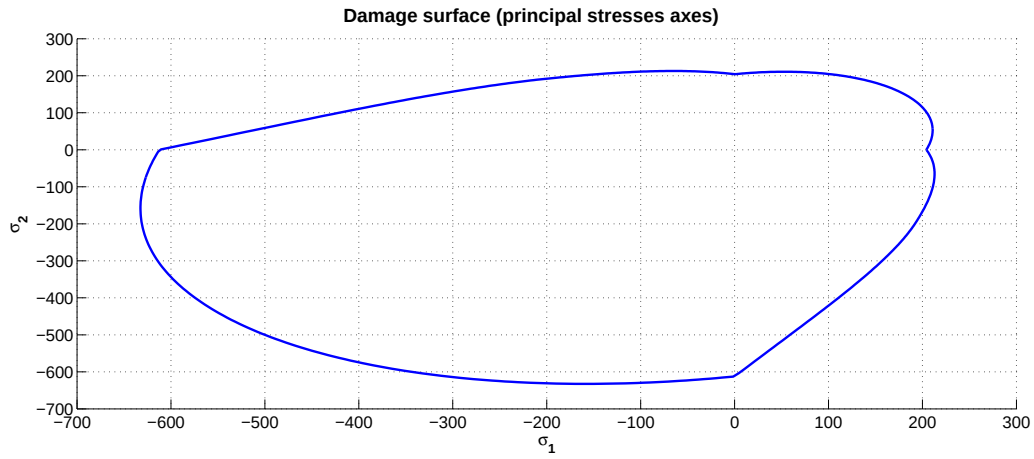

Figure 1: Damage surface/ Failure domain for the implemented non-symmetric tension-compression damage model

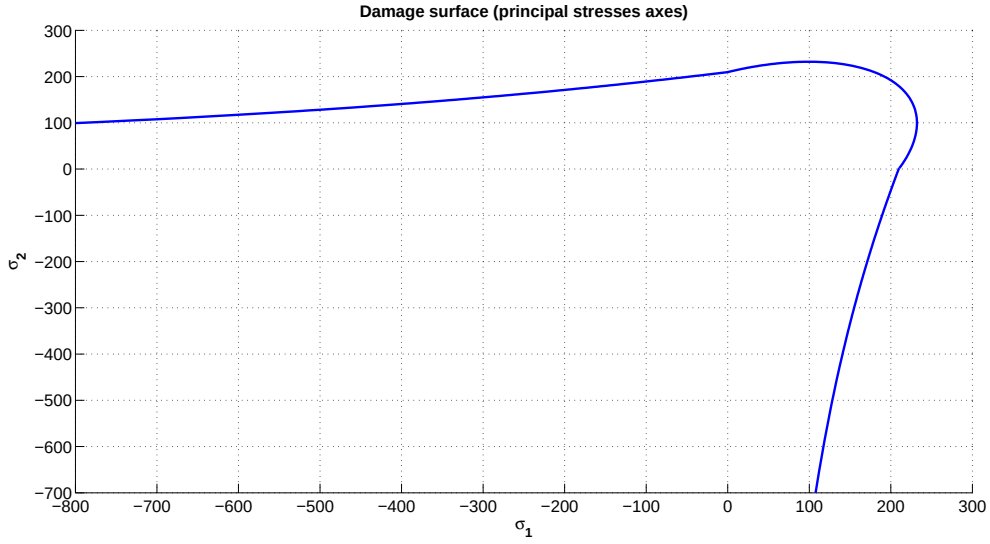

Figure 2: Damage surface/ Failure domain for the implemented Tensile-damage model

The continuum isotropic "symmetric tension-compression damage" model:

This type of damage model is useful, when the material behaves the same both with tension and compression. The damage surface evolves symmetrically both for tension and compression. For this type of damage models, in contrast to the other two discussed damage models, the elastic domain is symmetrically located for both the tensile and compressive stresses. The material loses elasticity both due to tension and compression.

(b) Exponential hardening/softening:

It can be considered as a type of continuous Hardening/Softening unlike having two sections (*i.e.* $H = Constant\ for\ r < r_1\ and\ H = 0\ for\ r > r_1$) as it was for the linear hardening/softening. An exponential hardening/softening model has been implemented choosing a suitable value for q_∞.

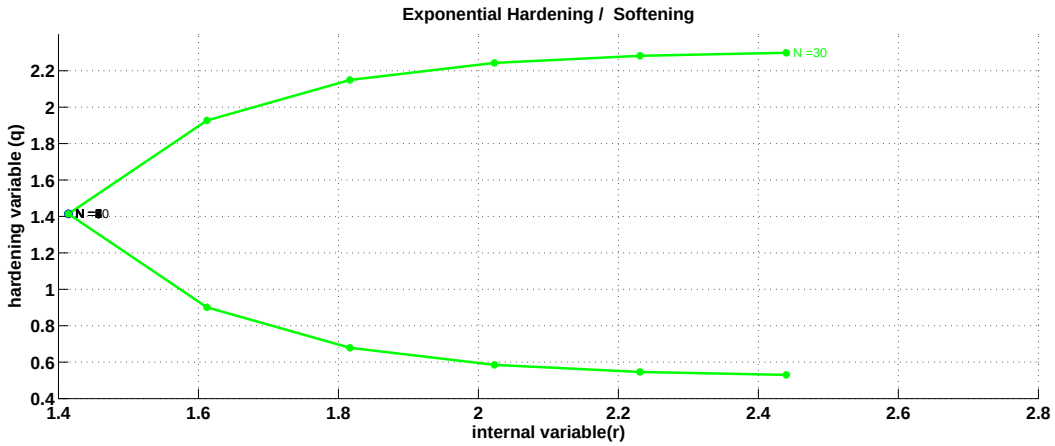

Figure 3: Variation of q vs. r in the implemented Exponential hardening/softening model

The value of q_∞ can never be negative as it will cause the size of the elastic domain to be negative,which is not feasible. If $q_\infty = 0$, at the end, elastic domain might shrink to zero and it can create problems in structural level but can work well in microscopic damage level. A very large value of the q_∞ is also not feasible as it affects the algorithmic constitutive tensor. For the implemented model, when $r \to \infty, q \to q_\infty$. In the case of hardening the $q_\infty > r_0$, and for the case of softening $q_\infty < r_0$. The Figure 3 represented above shows the variation of q with respect to r for the considered cases where $H = 6$ for hardening and $H = -6$ for softening. The implemented code has been presented in the Section 3 of the Annex.

(c) Accessing the correctness of the implementation of the models:

Case 1

$$(\Delta\bar{\sigma_1}^{(1)} = \alpha,\ \Delta\bar{\sigma_2}^{(1)} = 0), (\Delta\bar{\sigma_1}^{(2)} = -\beta,\ \Delta\bar{\sigma_2}^{(2)} = 0),\ (\Delta\bar{\sigma_1}^{(3)} = \gamma,\ \Delta\bar{\sigma_2}^{(3)} = 0)$$

"Non-symmetric tension-compression damage" model:

$$(\Delta\bar{\sigma_1}^{(1)} = 600,\ \Delta\bar{\sigma_2}^{(1)} = 0), (\Delta\bar{\sigma_1}^{(2)} = -2700,\ \Delta\bar{\sigma_2}^{(2)} = 0),\ (\Delta\bar{\sigma_1}^{(3)} = 2100,\ \Delta\bar{\sigma_2}^{(3)} = 0)$$

The material is loaded from the initial effective principal stress state (0, 0) to (600, 0) (uni-axial tensile loading), after which the uni-axial tensile unloading/compressive loading takes place till the effective principal stress state reaches (-2100, 0), and following that at the end the material is subjected to uni-axial compressive unloading/ tensile loading up till the effective principal stress state reaches (0, 0). The hardening modulus has been considered to be -0.2 (linear softening). At the starting, till the stress state reaches the elastic domain the effective and the actual stresses are same (N=1 to N=5)due to no evolution of the internal variables inside the elastic domain. After which when the stress path leaves the elastic domain, the stresses are projected back on to the evolved damage surface (N=5 to N=11). This case corresponds to the case of loading ($\dot{d} > 0$), as we consider $H < 0$, the elastic domain shrinks inwards and the stresses are projected on to the new evolved damage surfaces. Following this when the unloading occurs ($\dot{d} = 0$), the actual stress path tends along a straight line with slope $E^{(Sec-d)} = (1 - d_1)E$ along the secant constitutive path that passes through the origin. The actual stress path continues to be along on the same line till the stress state reaches the elastic limit for the compression which is higher than that of the elastic limit due to tension for this non-symmetric model

(N=11 to N=19). After which, when the stress path leaves the elastic limit of compression, again this case becomes the case of loading and also the elastic domain shrinks inwards and the stresses are projected back by the integration algorithm on to the new evolved damage surface (N=19 to N=20). Following this the uni-axial elastic tensile loading occurs. The actual stress path again becomes along another straight line with a slope $E^{(Sec-d)} = (1 - d_2)E$, along the secant constitutive path, with the new current value of the damage variable $d = d_2$, till it reaches the origin, where the final stress state reaches (0, 0) (N=20 to N=30). The evolution of the damage surface in the stress space has been shown in the Figure 4 for this considered loading path. The above explained phenomenon can be observed from the Figure 5 below in which the principal stress 1(Which is same as Stress for this uni-axial case) is plotted vs. the principal strain 1 (same as Strain for the uni-axial case).

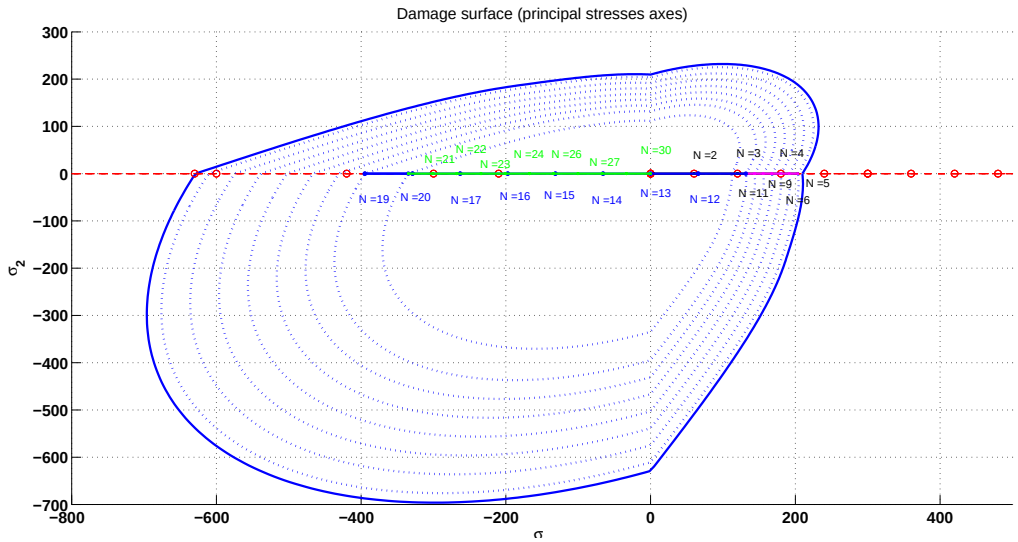

Figure 4: Path at the stress space for the "Non-symmetric tension-compression damage" model

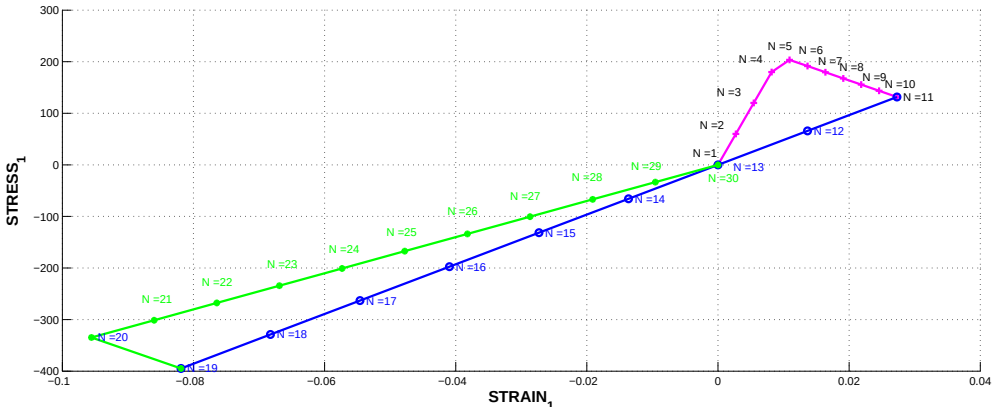

Figure 5: The stress-strain curve for the uni-axial "Non-symmetric tension-compression damage" model

The "tension-only" damage model:

$$(\Delta\bar{\sigma_1}^{(1)} = 400,\ \Delta\bar{\sigma_2}^{(1)} = 0), (\Delta\bar{\sigma_1}^{(2)} = -1000,\ \Delta\bar{\sigma_2}^{(2)} = 0),\ (\Delta\bar{\sigma_1}^{(3)} = 600,\ \Delta\bar{\sigma_2}^{(3)} = 0)$$

The material is loaded from the initial effective principal stress state (0, 0) to (400, 0) (uni-axial tensile loading), after which the uni-axial tensile unloading/compressive loading takes place till the effective principal stress state reaches (-600, 0), and following this at the end the material is subjected to uni-axial compressive unloading/ tensile loading up till the effective principal stress state reaches (0, 0). The hardening modulus has been considered to be -0.2 (linear softening). At the starting,

till the stress state reaches the elastic domain the effective and the actual stresses are same (N=1 to N=6). After which when the stress path leaves the elastic domain, the stresses are projected back on to the evolved damage surface (N=6 to N=11). This case corresponds to the case of loading ($\dot{d} > 0$), as we consider $H < 0$, the elastic domain shrinks inwards and the stresses are projected on to the new damage surface. Following this when the unloading occurs ($\dot{d} = 0$), the actual stress path trends along a straight line with slope $E^{(Sec-d)} = (1 - d_1)E$ along the secant constitutive path that passes through the origin. The actual stress path continues to be along on the same line throughout till the effective stress path reaches (-600, 0), as we can't find the elastic limit in compression up to infinite. In this case the elastic domain is an open domain at infinite for compressive stresses ($\dot{d} = 0$) (N=11 to N=20). The elastic domain also does not evolve as the stress path does not cross the elastic limit for compression which is at the infinite. Following this when the uni-axial elastic tensile loading occurs till the effective stress state reaches (0, 0), the actual stress path again follows the same straight line having the same slope $E^{(Sec-d)} = (1 - d_1)E$ in the opposite direction towards the origin till the stress state reaches (0,0) (N=20 to N=30). The evolution of the damage surface in the stress space has been shown in the Figure 6 for this considered loading path. The above explained phenomenon can be observed from the Figure 7 below in which the principal stress 1(Which is same as Stress for the uni-axial case) is plotted vs. the principal strain 1(same as Strain for the uni-axial case).

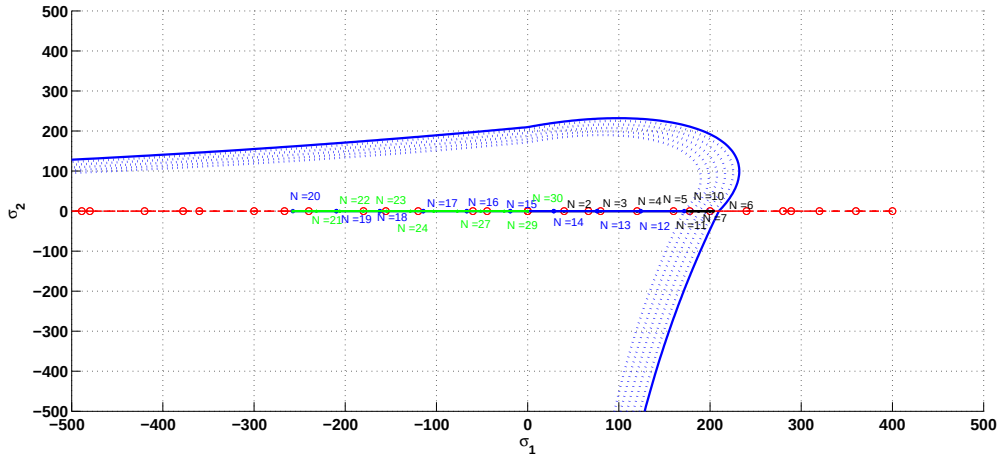

Figure 6: Path at the stress space for the "tension-only" damage model

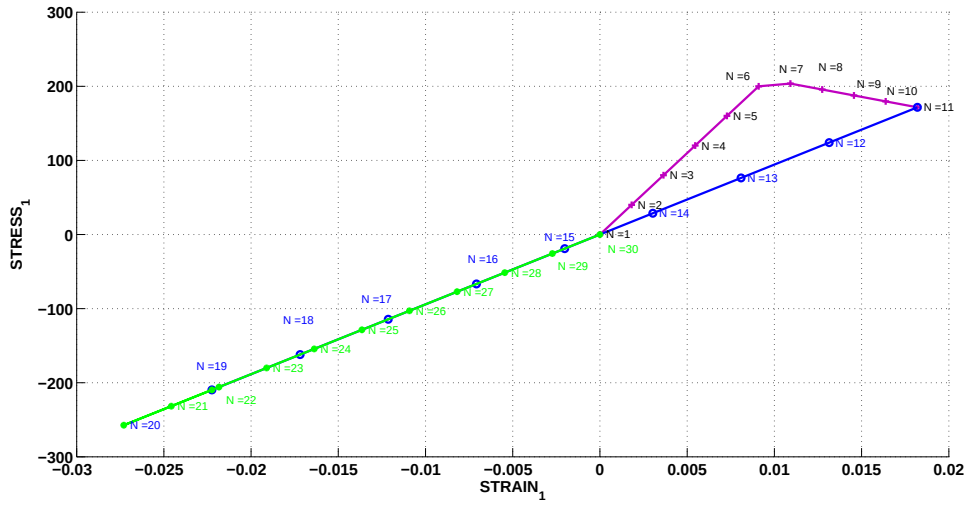

Figure 7: The stress-strain curve for the uniaxial "The tension-only damage model"

Case 2:

$$(\Delta\bar{\sigma_1}^{(1)} = \alpha,\ \Delta\bar{\sigma_2}^{(1)} = 0), (\Delta\bar{\sigma_1}^{(2)} = -\beta,\ \Delta\bar{\sigma_2}^{(2)} = -\beta),\ (\Delta\bar{\sigma_1}^{(3)} = \gamma,\ \Delta\bar{\sigma_2}^{(3)} = \gamma)$$

"Non-symmetric tension-compression damage" model:

$$(\Delta\bar{\sigma_1}^{(1)} = 300,\ \Delta\bar{\sigma_2}^{(1)} = 0), (\Delta\bar{\sigma_1}^{(2)} = -1000,\ \Delta\bar{\sigma_2}^{(2)} = -1000),\ (\Delta\bar{\sigma_1}^{(3)} = 1300,\ \Delta\bar{\sigma_2}^{(3)} = 1300)$$

The material is loaded from the initial effective principal stress state (0, 0) to (300, 0) (uni-axial tensile loading), after which the biaxial tensile unloading/compressive loading takes place till the effective principal stress state reaches (-700,-1000), and following this at the end, the material is subjected to biaxial compressive unloading/tensile loading up till the effective principal stress state reaches (600, 300). The hardening modulus has been considered to be 0. At the starting, during the uni-axial elastic loading, till the stress state reaches the elastic domain the effective and the actual stresses are same (N=1 to N=8). After which when the stress path leaves the elastic domain for tension, the stresses are projected back on to the evolved damage surface (N=8 to N=11). This case corresponds to the case of loading $(\dot{d} > 0)$. Following this when biaxial tensile unloading/compressive loading occurs, the actual stress follows the path shown in the figure from N=11 to N=12; and N =12 to N=17 till the stress path reaches the biaxial elastic limit for compression. After which, when the stress path leaves the elastic limit of compression, again this case becomes the case of loading and the stresses are projected back on to the damage surface (N=17 to N=20). After that, the biaxial compressive unloading/tensile loading takes place. Until the stress path reaches again the biaxial tensile elastic limit the actual stress path follows as shown in the figure from N=20 to N=29. After which when the stress path leaves the elastic domain for tension, the stresses are projected back on to the damage surface (N=29 to N=30). The evolution of the damage surface in the stress space has been shown in the Figure 8 for this considered loading path.

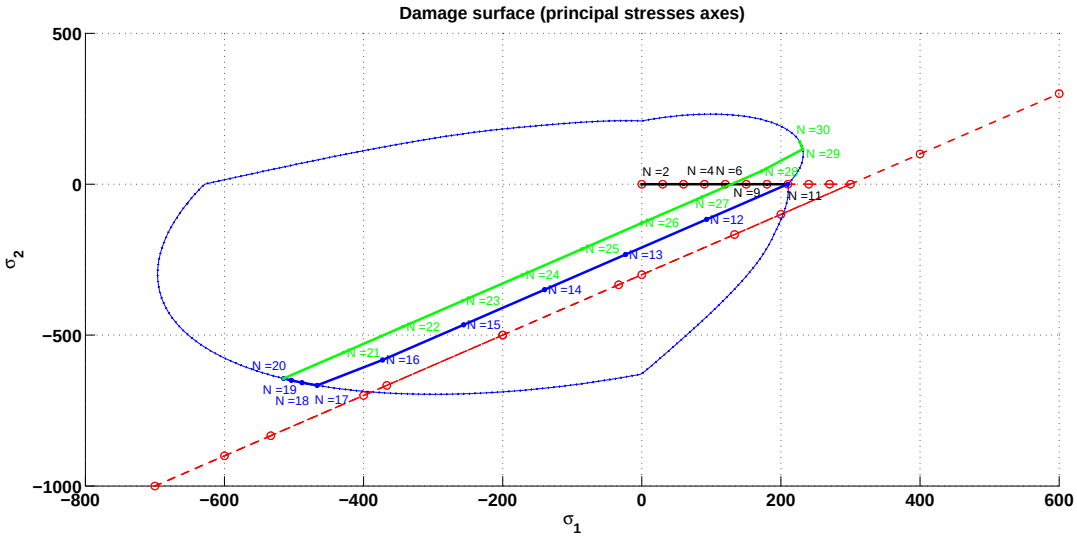

Figure 8: Path at the stress space for the "Non-symmetric tension-compression damage" model for the Case 2

The above explained phenomenon can be observed from the Figure 9 below in which the norm of stresses is plotted vs. the norm of the strains.

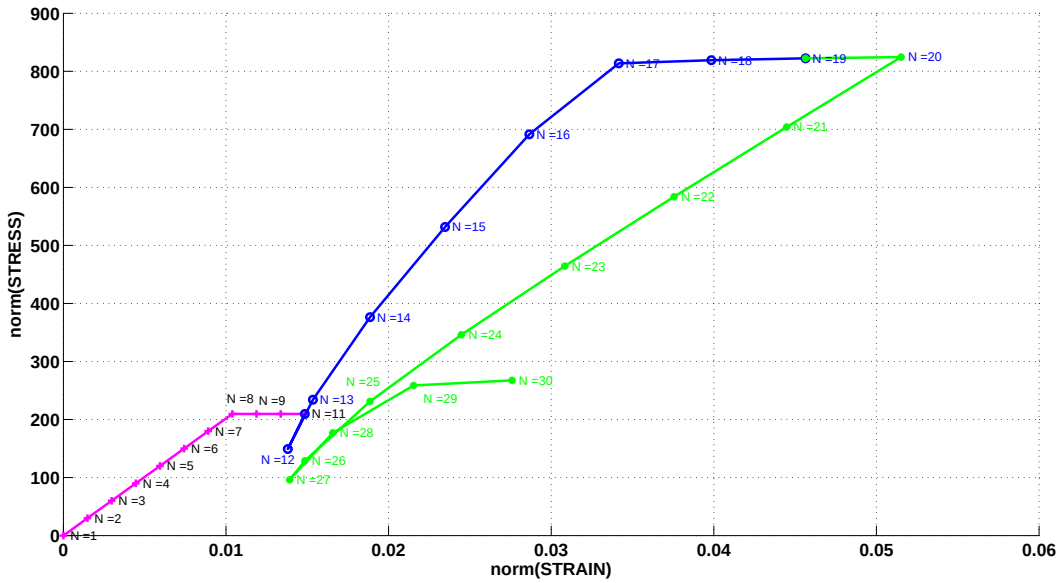

Figure 9: The stress-strain curve for the biaxial "Non-symmetric tension-compression damage" model (Case 2)

The "tension-only" damage model :

$$(\Delta\bar{\sigma_1}^{(1)} = 400,\ \Delta\bar{\sigma_2}^{(1)} = 0), (\Delta\bar{\sigma_1}^{(2)} = -600,\ \Delta\bar{\sigma_2}^{(2)} = -600),\ (\Delta\bar{\sigma_1}^{(3)} = 800,\ \Delta\bar{\sigma_2}^{(3)} = 800)$$

The material is loaded from the initial effective principal stress state (0, 0) to (400, 0) (uniaxial tensile loading), after which the biaxial tensile unloading/compressive loading takes place till the effective principal stress state reaches (-200,-600), and following this at the end the material is subjected to biaxial compressive unloading/tensile loading up till the effective principal stress state reaches (600, 200). The hardening modulus has been considered to be 0. At the starting, during the uni-axial elastic loading, till the stress state reaches the tensile elastic domain the effective and the actual stresses are same (N=1 to N=6). After which when the stress path leaves the elastic domain for tension, the stresses are projected back on to the evolved damage surface (N=6 to N=11). This case corresponds to the case of loading ($\dot{d} > 0$). Following this when biaxial tensile unloading/compressive loading occurs, the actual stress follows the path shown in the figure from N=11 to N=14 and then N=14 to N=20; as the biaxial elastic limit due to compression can never be reached. After that, the biaxial compressive unloading/tensile loading takes place. Until the stress path reaches again the biaxial tensile elastic limit, the actual stress path follows as shown in the figure from N=20 to N=27. After which when the stress path leaves the elastic domain for tension, the stresses are projected back on to the damage surface (N=27 to N=30). The evolution of the damage surface in the stress space has been shown in the Figure 10 for this considered loading path. The above explained phenomenon can be observed from the Figure 11 below in which the norm of stresses is plotted vs. the norm of the strains.

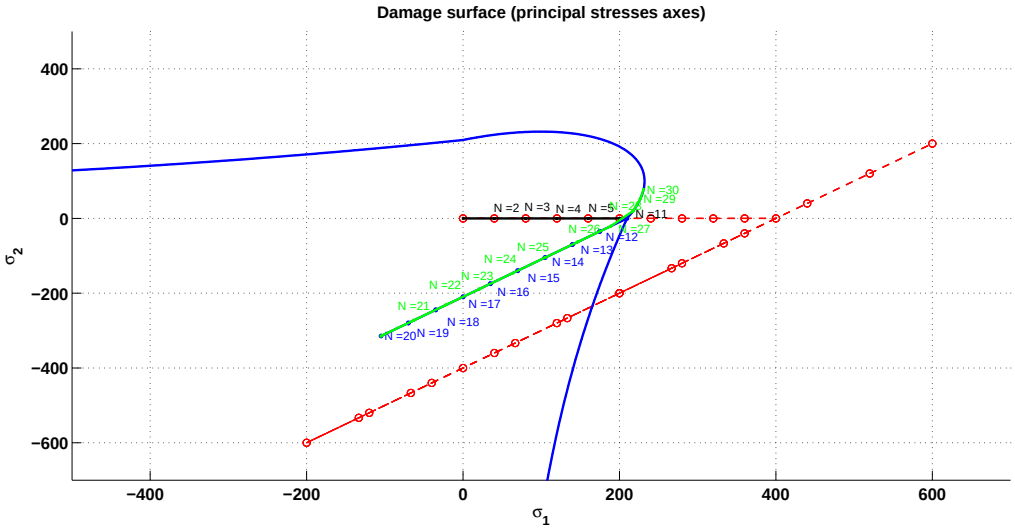

Figure 10: Path at the stress space for the "tension-only" damage model for Case 2

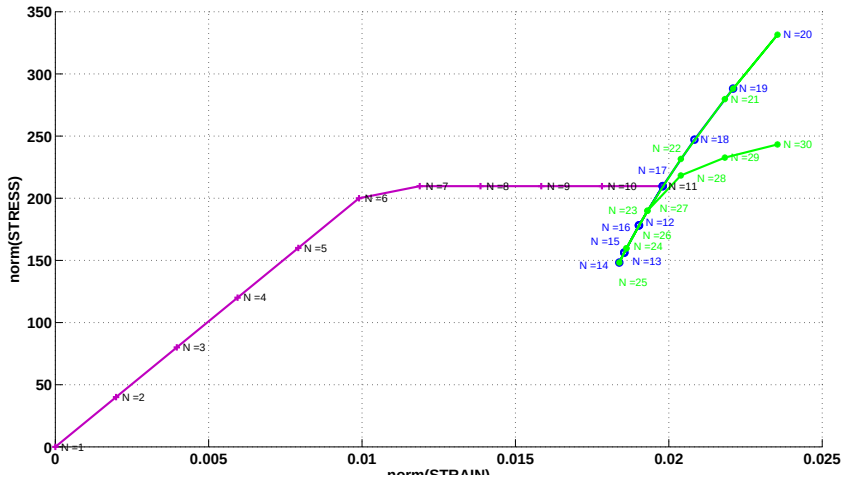

Figure 11: The stress-strain curve for the biaxial "The tension-only damage model" (Case 2)

Case 3:

$$(\Delta\bar{\sigma_1}^{(1)} = \alpha,\ \Delta\bar{\sigma_2}^{(1)} = \alpha), (\Delta\bar{\sigma_1}^{(2)} = -\beta,\ \Delta\bar{\sigma_2}^{(2)} = -\beta),\ (\Delta\bar{\sigma_1}^{(3)} = \gamma,\ \Delta\bar{\sigma_2}^{(3)} = \gamma)$$

"Non-symmetric tension-compression damage" model:

$$(\Delta\bar{\sigma_1}^{(1)} = 400,\ \Delta\bar{\sigma_2}^{(1)} = 400), (\Delta\bar{\sigma_1}^{(2)} = -2000,\ \Delta\bar{\sigma_2}^{(2)} = -2000),\ (\Delta\bar{\sigma_1}^{(3)} = 1600,\ \Delta\bar{\sigma_2}^{(3)} = 1600)$$

The material is loaded from the initial effective principal stress state (0, 0) to (400, 400) (biaxial tensile loading), after which the biaxial tensile unloading/compressive loading takes place till the effective principal stress state reaches (-1600,-1600), and following this at the end the material is subjected to biaxial compressive unloading/tensile loading up till the effective principal stress state reaches (0, 0). The hardening modulus has been considered to be 0.2 with the considered case of the linear hardening. At the starting, during the biaxial elastic loading, till the stress state reaches the elastic domain due to tension, the effective and the actual stresses are same (N=1 to N=6). After which when the stress path leaves the elastic domain for tension, the stresses are projected back on to the new evolved damage surface (N=6 to N=11). As,$H > 0$, the damage surface expands. This case

corresponds to the case of loading ($\dot{d} > 0$). Following this when biaxial tensile unloading/compressive loading occurs, the actual stress follows the secant path shown in the figure from N=11 to N=13 and passes through the stress state (0, 0); and it moves along the same straight line(from N =13 to N=18) till the stress state reaches the biaxial compressive elastic limit. After which, when the stress path leaves the elastic limit of compression, again this case becomes the case of loading and the stresses are projected back on to the new evolved damage surface due to hardening (N=18 to N=20). As, $H > 0$, the damage surface expands. Following this, the biaxial compressive unloading/tensile loading takes place($\dot{d} = 0$). The stress path follows the secant path along the same straight line but in the opposite direction till it reaches (0, 0). It is shown from N=20 to N=30. The evolution of the damage surface in the stress space has been shown in the Figure 12 for this considered loading path. The above explained phenomenon can be observed from the Figure 13 below in which the norm of stresses is plotted vs. the norm of the strains.

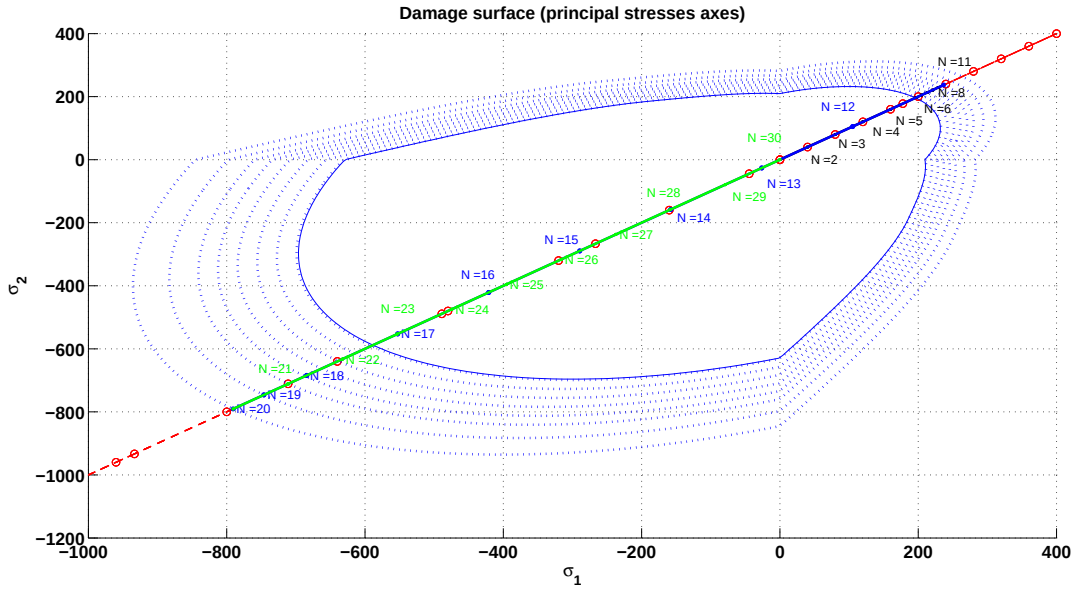

Figure 12: Path at the stress space for the "Non-symmetric tension-compression damage" model for the Case 3

The "tension-only" damage model:

$(\Delta\bar{\sigma_1}^{(1)} = 400,\ \Delta\bar{\sigma_2}^{(1)} = 400), (\Delta\bar{\sigma_1}^{(2)} = -900,\ \Delta\bar{\sigma_2}^{(2)} = -900),\ (\Delta\bar{\sigma_1}^{(3)} = 500,\ \Delta\bar{\sigma_2}^{(3)} = 500)$

The material is loaded from the initial effective principal stress state (0, 0) to (400, 400) (uniaxial tensile loading), after which the biaxial tensile unloading/compressive loading takes place till the effective principal stress state reaches (-500,-500), and following this at the end the material is subjected to biaxial compressive unloading/tensile loading up till the effective principal stress state reaches (0, 0). The hardening modulus has been considered to be 0.2 with the considered case of the linear hardening. At the starting, during the uniaxial elastic loading, till the stress state reaches the tensile elastic domain the effective and the actual stresses are same (N=1 to N=6). After which when the stress path leaves the elastic domain for tension, the stresses are projected back on to the evolved damage surface (N=6 to N=11).

This case corresponds to the case of loading ($\dot{d} > 0$). Following this when biaxial tensile unloading/compressive loading occurs, the actual stress follows the secant path shown in the figure from N=11 to N=15 till it reaches origin and then N=15 to N=20; as the biaxial elastic limit due to compression can never be reached. Following this, the biaxial compressive unloading/tensile loading takes place. The stress path follows the same straight line as this is the case of elastic unloading ($\dot{d} = 0$)

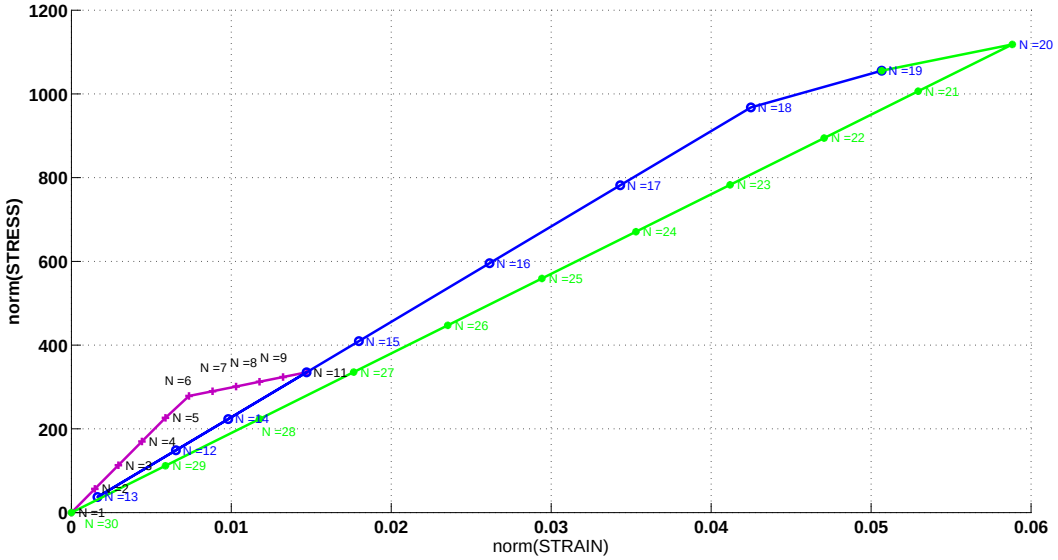

Figure 13: The stress-strain curve for the biaxial "Non-symmetric tension-compression damage" model (Case 3)

till the stress state reaches origin. It is shown in the figure below from N=20 to N=30. The evolution of the damage surface in the stress space has been shown in the Figure 14 for this considered loading path. The above explained phenomenon can be observed from the Figure 15 below in which the norm of stresses is plotted vs. the norm of the strains.

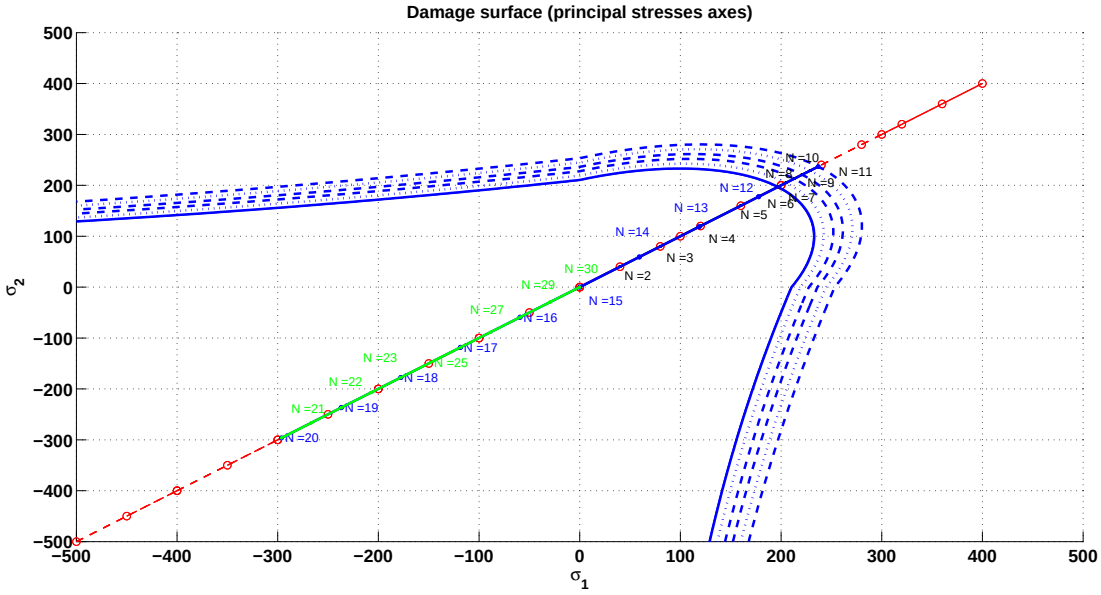

Figure 14: Path at the stress space for the "tension-only" damage model for Case 3

The above observations verify the correctness of the implemented damage models.

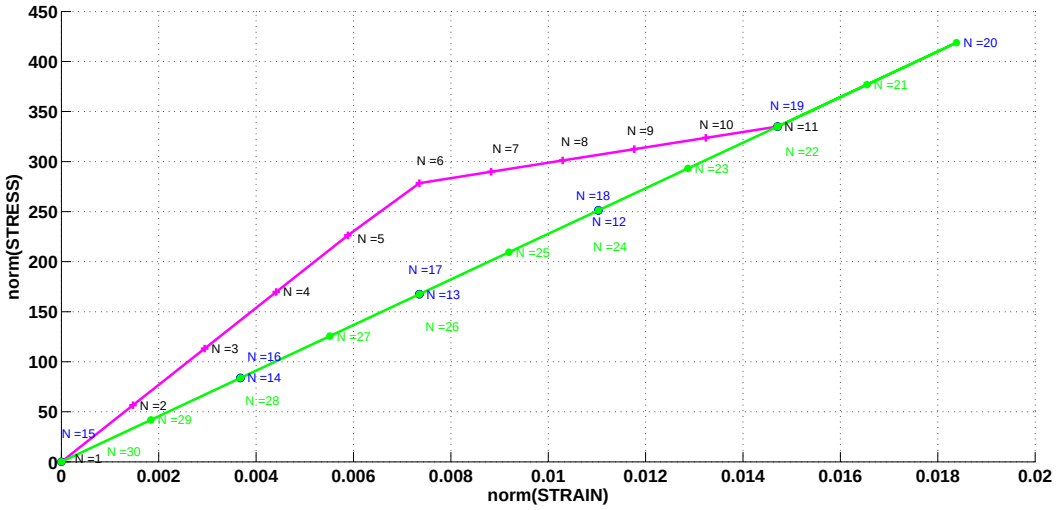

Figure 15: The stress-strain curve for the biaxial "The tension-only damage model" (Case 3)

Part 2:

(d) Visco-damage "symmetric tension compression" model:

The integration algorithm (plane strain case) for the continuum isotropic viscous-damage "symmetric tension compression" model has been implemented successfully. The code is presented in the Section 4 of the Annex. In this type of models the rate effects are accommodated into the in-viscid damage model. The stresses become dependent on both the strains and the rate of the strains. When the strain rate is very low, it coincides with the case of inviscid ($\eta = 0$) case. In this type of models, the stress/strain state can lie outside the elastic domain. When the coefficient of viscosity is very high, points can leave far away from the elastic domain. When the state of the effective stresses lie inside the elastic domain, there is no evolution of the internal variables takes place. It is similar to that of the in-viscid model. When the state of the effective stresses lie outside the elastic domain, the actual stress state might lie outside the elastic domain depending open the value of the viscosity. The evolution of the stress space is shown in the Figure 16 for the observed case. It can be observed that the state of the actual stresses can lie outside the elastic domain in the viscid case. For this observation the effective stress path is chosen such that:

$$(\Delta\bar{\sigma_1}^{(1)} = 100,\ \Delta\bar{\sigma_2}^{(1)} = 0), (\Delta\bar{\sigma_1}^{(2)} = 400,\ \Delta\bar{\sigma_2}^{(2)} = 0),\ (\Delta\bar{\sigma_1}^{(3)} = -500,\ \Delta\bar{\sigma_2}^{(3)} = 0)$$

The viscosity value has been taken $\eta = 10$, and other parameters are set as $\alpha = 5, \gamma = 0.3, H = 0.2$ (*Linear Hardening*). The actual stress states, from N=8 to N=14, lie outside the elastic domain. When the effective stress states lie in the elastic domain, as no evolution of the internal variable take place, the actual stresses become same as that of the effective stresses (N1 to N7). It can be observed from the Figure 17 where the norm of the stresses are plotted vs. the norm of the strains.

Another characteristic of this type of model is that the stress tensor might vary even if ε remains constant while for inviscid models the stress tensors remains constant if strain remains constant. This property has been shown in the Figure 18, where along the path N=21 to N=30 effective strain remains constant by choosing the effective stress path such that $(\Delta\bar{\sigma_1}^{(1)} = 100,\ \Delta\bar{\sigma_2}^{(1)} = 0), (\Delta\bar{\sigma_1}^{(2)} = 400,\ \Delta\bar{\sigma_2}^{(2)} = 0),\ (\Delta\bar{\sigma_1}^{(3)} = 0,\ \Delta\bar{\sigma_2}^{(3)} = 0)$; The viscosity value has been taken $\eta = 10$, and other parameters are set as $\alpha = 0.5, \nu = 0.3, H = -0.025$.

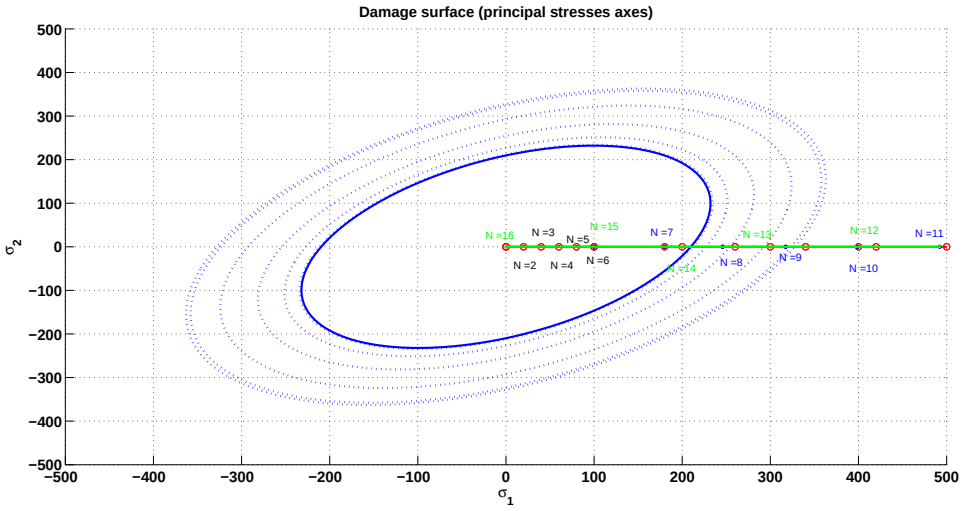

Figure 16: The evolution of the actual stresses for a viscous damage model

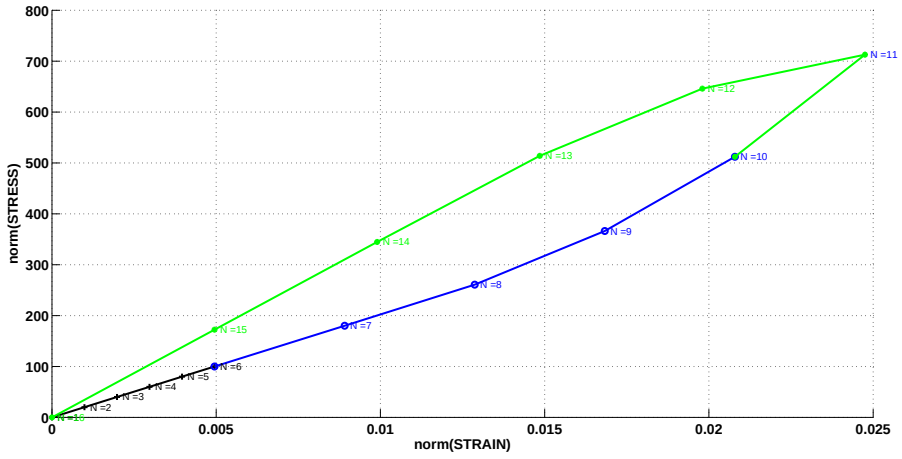

Figure 17: Norm of stresses vs. norm of strains for a viscous damage model

(e) Effect of Different viscosity parameters η:

It is observed that outside the elastic region the larger are the viscosity parameters η, the larger are the stresses for the same strain value. In the elastic part, there are no differences and the stresses are independent of the viscosity parameters η. It can be observed from the Figure 19, where stress norms are plotted vs. strain norms for different values of viscosity parameters η. For the observed case, the considered parameters are: $\alpha = 0.5, H = -0.025$ $(LinearSoftening); \nu = 0.3$, The effective stress path trends: (100,0),(300,0),(600,0)

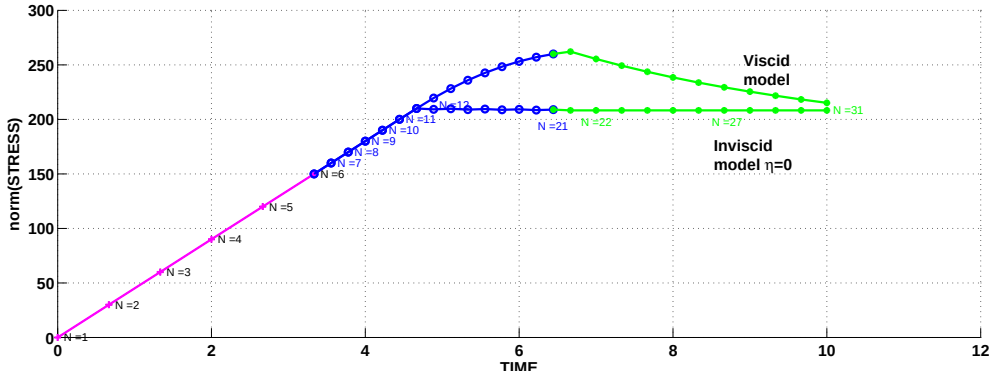

Figure 18: Comparison of the evolution of stresses with time for constant strain for viscid and non-viscid models.

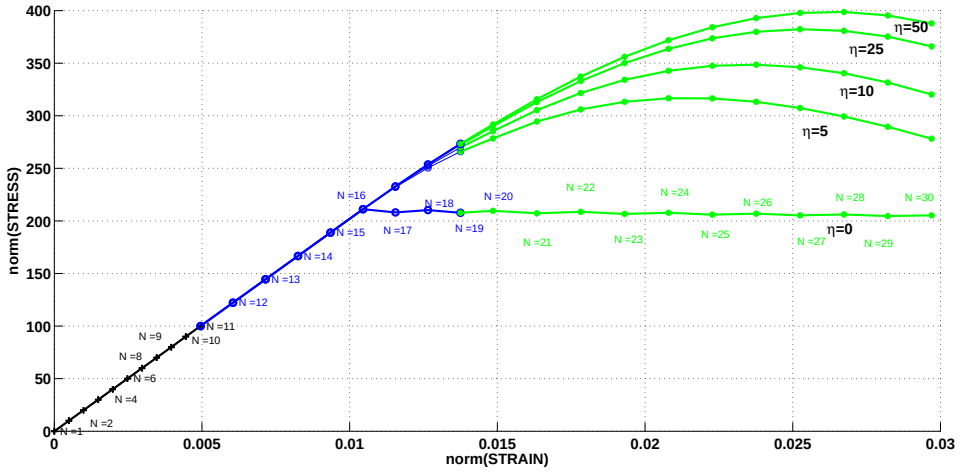

Figure 19: Variation of Stress vs. Strain for different values of the viscosity parameter η

Effect of different strain rates:

It is observed that outside the elastic region the larger are the strain rate values, the larger are the stresses for the same strain value. In the elastic part, there are no differences and the stresses are independent of the values of the strain rates due to the no evolution of the internal variables. It can be observed from the Figure 20 , where stress norms are plotted vs. strain norms for different values of the strain rates. For the observed case the considered parameters are: $\alpha = 0.5, H = -0.025$ $(LinearSoftening); \gamma = 0.3, \eta = 5$. The effective stress path: (100,0); (200,0); (300,0). When the viscosity parameter,η =0, all the strain rate curves collapse in to the curve which corresponds to the strain rate value of zero.

Effect of different alpha values:

The Effect of different alpha values on the accuracy and the stability of the numerical integration have been studied. For the observed case the considered parameters are: $H = 0; \nu = 0.3, \eta = 10$. The considered effective stress path: (200, 0); (400,0); (700,0).The observations are depicted in the stress-strain plot below. It is observed that for α=0 the numerical integration scheme is conditionally stable, and this explicit method gives first order accuracy. With the larger time step size, this scheme becomes unstable. This observation is shown in the Figure 21, below for a large considered time step value. The similar effects are also observed for α= 0.25.

This explicit scheme (α= 0.25) gives first order accuracy and it is conditionally stable and the

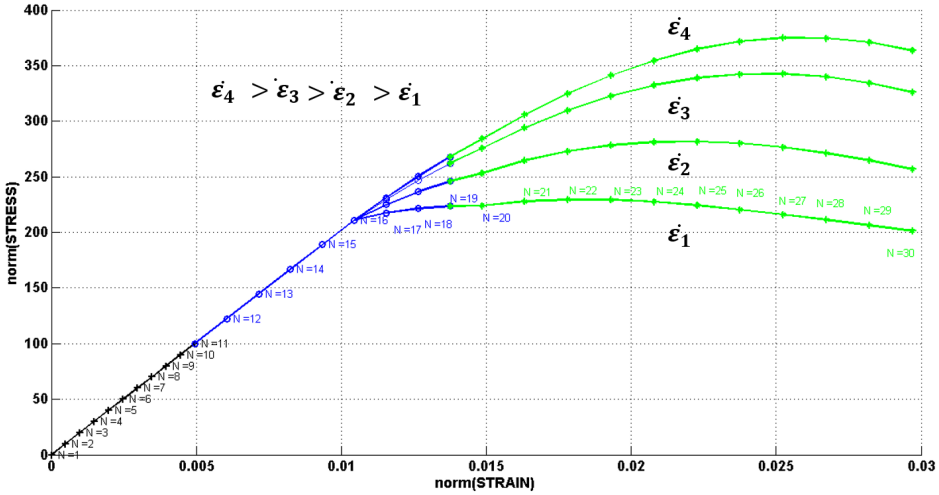

Figure 20: Variation of Stress vs. Strain for different values of the strain rates η

stability depends on the size of the time-step. For α= 0.5, the numerical scheme is unconditionally stable and it gives second order accuracy. In this case the solution converges faster to the exact solution than all other alpha values in$[0, 1]$. The error does not propagate for any values of the time step in this case. For α= 0.75, the numerical scheme is unconditionally stable and it gives first order accuracy. For α= 1, the numerical scheme is unconditionally stable and it gives first order accuracy. It is an implicit scheme. For α= 1 and η=0, Numerical integration inherits the properties of the model and recovers the solution of the rate independent problem for the in viscid case and implicit integration. Inside the elastic region, all the integration schemes corresponding to the different values of α give same result. For a small time step value, all the alpha methods give similar results with significantly small variations.

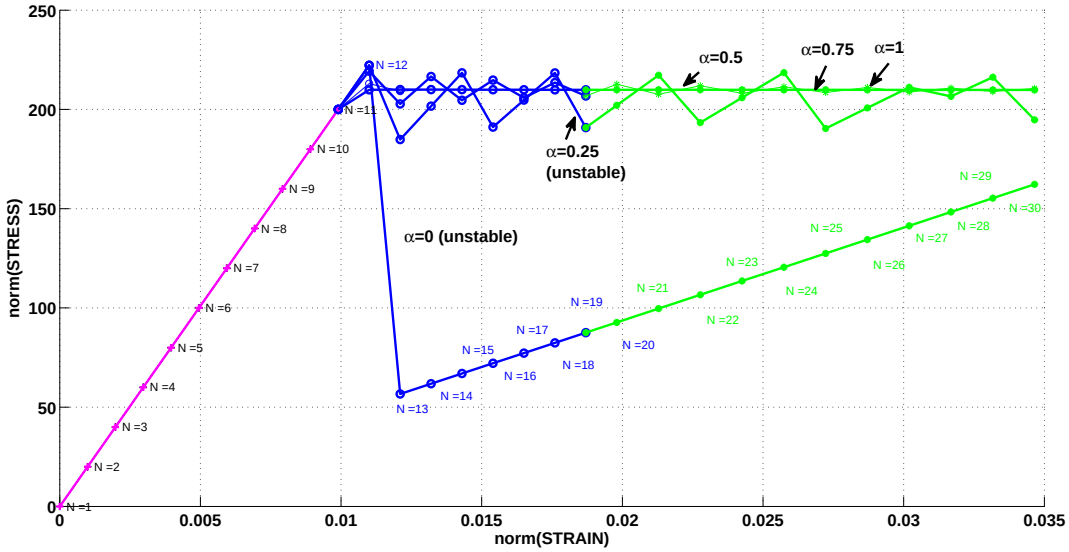

Figure 21: Stress vs. Strain plot for different values of α for a large time step-size

Effect of α on the evolution of the C11 component of the tangent and algorithmic constitutive operators along time:

The evolution of the C11 component of the tangent and algorithmic constitutive operators along the time has been studied for the different values of the α. The other considered parameters during

the observation are: H= -0.025 (Linear Softening),$\nu = 0.3, \eta = 10$. The considered effective stress path: (100,0); (300,0); (600,0). It is observed that in the elastic domain no evolution takes place for the C11 component of both the tangent and algorithmic constitutive operators along the time due to the no evolutions of the internal variables in that regime. Outside the elastic domain it is observed that for higher alpha values at a particular time, the values of the C11 component of the tangent and algorithmic constitutive operators gets reduced. The reduction is more for the algorithmic constitutive operators than the tangent constitutive operators at a particular time. When we consider α =0; both have same value and both trend same path along the time. These observations can be depicted from the Figures below. Also for infinitesimal time steps ($\delta t = 0$), they are equal. When $\eta = 0$ in the algorithmic constitutive operators, the in-viscid case is recovered for any values of the α.

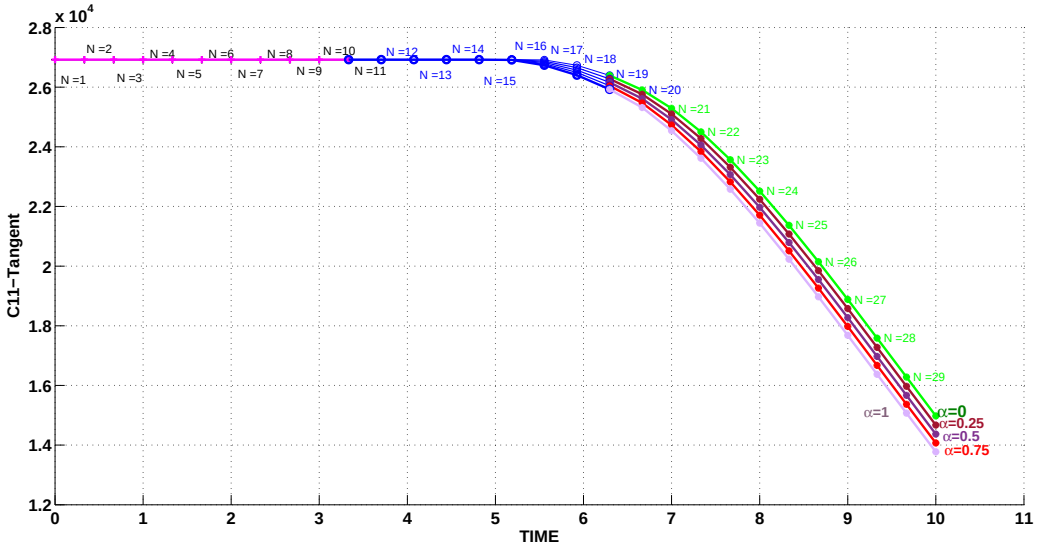

Figure 22: Evolution of the C11 component of the tangent constitutive operators along time for the different values of α

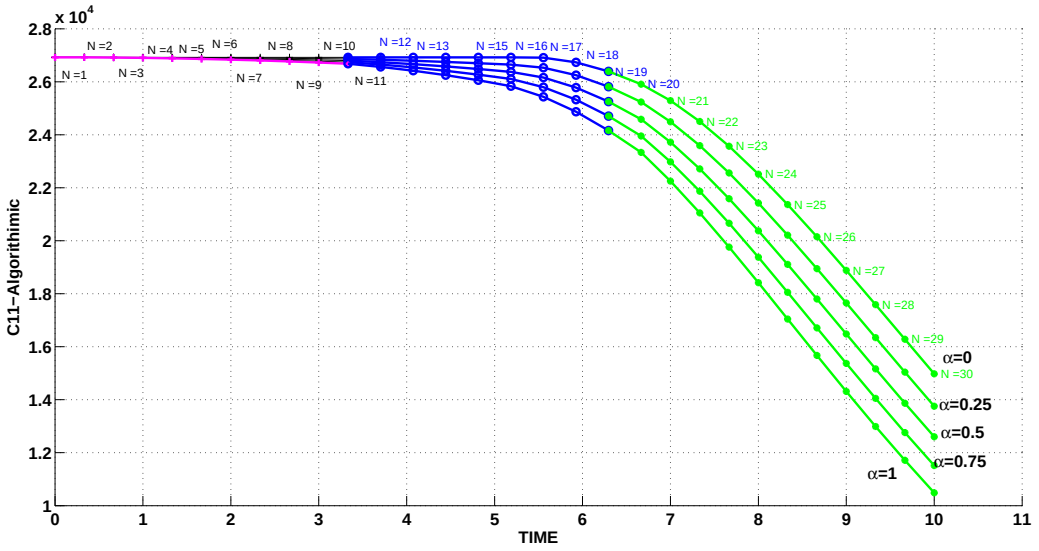

Figure 23: Evolution of the C11 component of the algorithmic constitutive operators along time for the different values of α

ANNEX:

Modelos_de_dano1.m: (Code: Section 1 and 2)

```
if (MDtype==1)      % Symmetric (Already implemented)

    rtrial= sqrt(eps_n1*ce*eps_n1');

elseif (MDtype==2)  % Tension only Damage model

    sigmab=(eps_n1*ce);
    sigmabpos=sigmab.*(sigmab>0);

    rtrial=sqrt(sigmabpos*eps_n1');

elseif (MDtype==3)  %Non-symmetric Tension- Compression

    sigma=(eps_n1*ce);
    sigmapos=sigma.*(sigma>0);
    sigmaabs=abs(sigma);
    tita=sum(sigmapos)/sum(sigmaabs);
    C=(tita+(1-tita)/n);
    rtrial= C*sqrt(eps_n1*ce*eps_n1');

end
return
```

dibujar_criterio_dano1.m

```
elseif MDtype==2
    tetha=[(-pi/2)*0.9999:0.01:pi*0.9999]; % Angle

    %* RADIUS
    D=size(tetha);
    m1=cos(tetha);
    m2=sin(tetha);
    Contador=D(1,2);

    radio = zeros(1,Contador) ;
    s1    = zeros(1,Contador) ;
    s2    = zeros(1,Contador) ;

    for i=1:Contador
        sigma= [m1(i) m2(i) 0 nu*(m1(i)+m2(i))];
        sigmapos=sigma.*(sigma>0);
        radio(i)= q/sqrt(sigmapos*ce_inv*sigma');

        s1(i)=radio(i)*m1(i);
        s2(i)=radio(i)*m2(i);

    end
    hplot =plot(s1,s2,tipo_linea);

elseif MDtype==3
    tetha=[0:0.01:2*pi];
```

```
    %* RADIUS
    D=size(tetha);
    m1=cos(tetha);
    m2=sin(tetha);
    Contador=D(1,2);


    radio = zeros(1,Contador) ;
    s1    = zeros(1,Contador) ;
    s2    = zeros(1,Contador) ;


    for i=1:Contador

        sigma=[m1(i) m2(i) 0 nu*(m1(i)+m2(i))];
        sigmapos=sigma.*(sigma>0);
        tita=sum(sigmapos)/sum(abs(sigma));

        radio(i)= (q/sqrt(sigma*ce_inv*sigma'))/(tita+(1-tita)/n);

        s1(i)=radio(i)*m1(i);
        s2(i)=radio(i)*m2(i);

    end
    hplot =plot(s1,s2,tipo_linea);

end
return
```

Section 3 , 4 (rmap_dano1.m)

```
hvar_n1 = hvar_n;
r_n     = hvar_n(5);
q_n     = hvar_n(6);
E       = Eprop(1);
nu      = Eprop(2);
H       = Eprop(3);
sigma_u = Eprop(4);
hard_type = Eprop(5) ;
eta = Eprop(7);
ALPHA_COEFF = Eprop(8);
HARDSOFT_MOD = Eprop(3);
%*       initializing
 r0 = sigma_u/sqrt(E);
 zero_q=1.d-6*r0;
%*Damage surface
[rtrial_n] = Modelos_de_dano1 (MDtype,ce,eps_n0,n); % (Viscous model)
[rtrial] = Modelos_de_dano1 (MDtype,ce,eps_n1,n);
[rtrial_nalpha]=(1-ALPHA_COEFF)*rtrial_n+ALPHA_COEFF*rtrial ;
%*
%*   --------->    fload=0 : elastic unload
%*   --------->    fload=1 : damage (compute algorithmic constitutive
tensor)         %*
fload=0;

if viscpr == 1
    if (rtrial_nalpha > r_n)
        %*   Loading
        fload=1;
        delta_r=rtrial_nalpha-r_n;
```

```
        r_n1=((eta-delta_t*(1-
ALPHA_COEFF))/(eta+ALPHA_COEFF*delta_t))*r_n+...
            (delta_t*rtrial_nalpha)/(eta+ALPHA_COEFF*delta_t);
        if hard_type == 0
            %  Linear
            q_n1= q_n+ H*delta_r;
        else
            %Exponential

            q_inf=r0+(r0-zero_q);
            if HARDSOFT_MOD>0
                q_n1=q_n+((H*(q_inf-r0)/r0)*exp(H*(1-
rtrial_nalpha/r0)))*delta_r;
            else
                q_n1=q_n+((H*(q_inf-r0)/r0)*(1/exp(H*(1-
rtrial_nalpha/r0))))*delta_r;
            end

        end

         if(q_n1<zero_q)
            q_n1=zero_q;
        end

    else
        %*     Elastic load/unload
        fload=0;
        r_n1= r_n  ;
        q_n1= q_n  ;


    end

else
    if(rtrial > r_n)
        %*   Loading

        fload=1;
        delta_r=rtrial-r_n;
        r_n1= rtrial  ;
        if hard_type == 0
            %  Linear
            q_n1= q_n+ H*delta_r;
        else
            %Exponential

            q_inf=r0+(r0-zero_q);
            if HARDSOFT_MOD>0
                q_n1=q_n+((H*(q_inf-r0)/r0)*exp(H*(1-rtrial/r0)))*delta_r;
            else
                q_n1=q_n+((H*(q_inf-r0)/r0)*(1/exp(H*(1-
rtrial/r0))))*delta_r;
            end
        end

        if(q_n1<zero_q)
            q_n1=zero_q;
        end
```

```
    else

        %*     Elastic load/unload
        fload=0;
        r_n1= r_n  ;
        q_n1= q_n  ;


    end

end

% Damage variable
dano_n1   = 1.d0-(q_n1/r_n1);
%  Computing stress
sigma_n1  =(1.d0-dano_n1)*ce*eps_n1';
hvar_n1(5)= r_n1 ;
hvar_n1(6)= q_n1 ;
%* Auxiliar
variables                                                              %*
aux_var(1) = fload;
aux_var(2) = q_n1/r_n1;
```

damage_main.m

```
LABELPLOT = {'hardening variable (q)','internal variable(r)','damage
variable (d)','C11-Tangent','C11-Algorithimic'};

E      = Eprop(1) ; nu = Eprop(2) ;
viscpr = Eprop(6) ;
sigma_u = Eprop(4);



if ntype == 1
    menu('PLANE STRESS has not been implemented yet','STOP');
    error('OPTION NOT AVAILABLE')
elseif ntype == 3
    menu('3-DIMENSIONAL PROBLEM has not been implemented yet','STOP');
    error('OPTION NOT AVAILABLE')
else
    mstrain = 4    ;
    mhist   = 6    ;
end

% if viscpr == 1
%     % Comment/delete lines below once you have implemented this case
%     % *****************************************************
%     menu({'Viscous model has not been implemented yet. '; ...
%         'Modify files "damage_main.m","rmap_dano1" ' ; ...
%         'to include this option'},  ...
%         'STOP');
%     error('OPTION NOT AVAILABLE')
% else
% end
```

```
totalstep = sum(istep) ;


% INITIALIZING GLOBAL CELL ARRAYS
% -------------------------------
sigma_v = cell(totalstep+1,1) ;
TIMEVECTOR = zeros(totalstep+1,1) ;
delta_t = TimeTotal./istep/length(istep) ;


% Elastic constitutive tensor
% ---------------------------
[ce]    = tensor_elastico1 (Eprop, ntype);
% Initz.
% -----
% Strain vector
% -------------
eps_n1  = zeros(mstrain,1);
% Historic variables
% hvar_n(1:4) --> empty
% hvar_n(5) = q --> Hardening variable
% hvar_n(6) = r --> Internal variable
hvar_n  = zeros(mhist,1)  ;

% INITIALIZING  (i = 1) !!!!
% ***********i*
i = 1 ;
r0 = sigma_u/sqrt(E);
hvar_n(5) = r0; % r_n
hvar_n(6) = r0; % q_n
eps_n1 = strain(i,:) ;
sigma_n1 =ce*eps_n1'; % Elastic
sigma_v{i} = [sigma_n1(1)  sigma_n1(3) 0;sigma_n1(3) sigma_n1(2) 0 ; 0 0
sigma_n1(4)];

nplot = 3 ;
vartoplot = cell(1,totalstep+1) ;
vartoplot{i}(1) = hvar_n(6) ; % Hardening variable (q)
vartoplot{i}(2) = hvar_n(5) ; % Internal variable (r)
vartoplot{i}(3) = 1-hvar_n(6)/hvar_n(5)  ; %  Damage variable (d)
vartoplot{i}(4) =(1-( 1-hvar_n(6)/hvar_n(5)))*ce(1,1) ;  %%C11 of tangent
vartoplot{i}(5)=(1-( 1-hvar_n(6)/hvar_n(5)))*ce(1,1)+
(Eprop(8)*delta_t)/(Eprop(7)+Eprop(8)*delta_t)...
    *(Eprop(3)*hvar_n(5)-hvar_n(6))/( hvar_n(5) *
hvar_n(5) )*sigma_v{i}(1,1)*sigma_v{i}(1,1)/(1-( 1-
hvar_n(6)/hvar_n(5)))^2; %C11 OF algorithm


for  iload = 1:length(istep)
    % Load states
    for iloc = 1:istep(iload)
        i = i + 1 ;
        TIMEVECTOR(i) = TIMEVECTOR(i-1)+ delta_t(iload) ;
        % Total strain at step "i"
        % ------------------------
        eps_n1 = strain(i,:) ;
        eps_n0 = strain(i-1,:) ;
```

```
        %*****************************************************************
********************
        %*      DAMAGE MODEL
        % %%%%%%%%%%%%%%%%%%%%%%%%%%%%%%%%%%%%%%%%%%%%%%%%%%%%%%%%%%%%%%%
%%%%%
        [sigma_n1,hvar_n,aux_var] =
rmap_dano1(eps_n1,eps_n0,hvar_n,Eprop,ce,MDtype,n,viscpr,delta_t);
        % PLOTTING DAMAGE SURFACE
        if(aux_var(1)>0)
            hplotSURF(i) = dibujar_criterio_dano1(ce, nu, hvar_n(6),
'r:',MDtype,n );
            set(hplotSURF(i),'Color',[0 0
1],'LineWidth',1)                          ;
        end

        % GLOBAL VARIABLES
        % ***************
        % Stress
        % ------
        m_sigma=[sigma_n1(1)  sigma_n1(3) 0;sigma_n1(3) sigma_n1(2) 0 ; 0 0
sigma_n1(4)];
        sigma_v{i} =  m_sigma ;

        % VARIABLES TO PLOT (set label on cell array LABELPLOT)
        % ----------------
        vartoplot{i}(1) = hvar_n(6) ; % Hardening variable (q)
        vartoplot{i}(2) = hvar_n(5) ; % Internal variable (r)
        vartoplot{i}(3) = 1-hvar_n(6)/hvar_n(5)  ; %  Damage variable (d)
        vartoplot{i}(4) =(1-( 1-
hvar_n(6)/hvar_n(5)))*ce(1,1) ;          %%C11 of Tangent
         vartoplot{i}(5)=(1-( 1-hvar_n(6)/hvar_n(5)))*ce(1,1)+
(Eprop(8)*delta_t)/(Eprop(7)+Eprop(8)*delta_t)...
    *(Eprop(3)*hvar_n(5)-hvar_n(6))/( hvar_n(5) *
hvar_n(5) )*sigma_v{i}(1,1)*sigma_v{i}(1,1)/((1-( 1-
hvar_n(6)/hvar_n(5))))^2;
% c11 of Algorithimic %C11 OF TANGENT
```

END